atmosphere

Article

Characters of Particulate Matter and Their Relationship with Meteorological Factors during Winter Nanyang 2021–2022

Miao Zhang [1,2,3,*], Shiyong Chen [1], Xingang Zhang [1], Si Guo [1], Yunuo Wang [1], Feifei Zhao [1], Jinhan Chen [1], Pengcheng Qi [1], Fengxian Lu [1], Mingchun Chen [4] and Muhammad Bilal [5,*]

1 Academy of Remote Sensing Technology and Application, Nanyang Normal University, Wolong Road No. 1638, Nanyang 473061, China
2 Key Laboratory of Natural Disaster and Remote Sensing of Henan Province, Nanyang Normal University, Wolong Road No. 1638, Nanyang 473061, China
3 Engineering Research Center of Environmental Laser Remote Sensing Technology and Application of Henan Province, Nanyang Normal University, Wolong Road No. 1638, Nanyang 473061, China
4 Teacher Education College, Beijing Language and Culture University, Xueyuan Road No. 15, Beijing 100083, China
5 School of Surveying and Land Information Engineering, Henan Polytechnic University, Jiaozuo 454000, China
* Correspondence: zm_liesmars@whu.edu.cn (M.Z.); muhammad.bilal@connect.polyu.hk (M.B.); Tel.: +86-151-3909-7793 (M.Z.)

Abstract: The purpose of this study is to investigate the air quality levels of Nanyang city according to Chinese air quality standards. Therefore, in this study, fine particulate matter ($PM_{2.5}$), coarse particulate matter (PM_{10}), and total suspended particulate (TSP) were analyzed from 19 November 2021 to 19 March 2022 in Nanyang city. The results show that the average concentrations of $PM_{2.5}$, PM_{10}, and TSP were 106.47 μg/m^3, 137.32 μg/m^3, and 283.40 μg/m^3, respectively. The numbers of days that meet the national secondary air quality standard of 24-h average concentrations were 29.75% for $PM_{2.5}$, 63.64% for PM_{10}, and 63.64% for TSP, indicating that most of the time, the air quality of Nanyang city remains polluted in winter, especially with more contributions of $PM_{2.5}$ compared to PM_{10} and TSP. The higher concentrations were observed between 07:00 and 08:00, suggesting that vehicular emissions can be a major cause of air pollution in Nanyang city. The results also show a significant positive correlation between particulate matter and relative humidity, and a weak correlation with temperature and wind speed, which suggests that higher relative humidity increases the formation of particulate matter. This study can provide theoretical support for the local government to formulate air pollution prevention and control policies for Nanyang city.

Keywords: aerosol; particulate matters; Nanyang city; meteorological factors; winter

check for updates

Citation: Zhang, M.; Chen, S.; Zhang, X.; Guo, S.; Wang, Y.; Zhao, F.; Chen, J.; Qi, P.; Lu, F.; Chen, M.; et al. Characters of Particulate Matter and Their Relationship with Meteorological Factors during Winter Nanyang 2021–2022. *Atmosphere* **2023**, *14*, 137. https://doi.org/10.3390/atmos14010137

Academic Editor: Kei Sato

Received: 11 December 2022
Revised: 30 December 2022
Accepted: 4 January 2023
Published: 8 January 2023

1. Introduction

Aerosols are suspended systems of liquid or solid particles in the atmosphere [1,2]. The aerodynamic diameter of aerosol particles usually ranges from 0.01 to 100 μm, and their shapes can be subspherical, flaky, needle-like, or irregular [3]. Aerosols affect climate mainly through several mechanisms: first, atmospheric aerosols directly affect climate by scattering and absorbing short-wave and long-wave radiation [4–7]; second, aerosols can act as cloud condensation nuclei and ice nucleating particles affecting cloud micro-physical characteristics, and cloud droplet number density, cloud phase, and cloud life cycle indirectly affect the climate system [8,9]; third, aerosol particles indirectly influence atmospheric chemical processes, thus changing other atmospheric components such as greenhouse gases [10–15]. Aerosols affect the climate as well as the surrounding ecological environment and human health [16]. With the advancement of scientific research, aerosols are closely related to many environmental problems such as haze and smog events [17,18]. The fine particulate matter $PM_{2.5}$ (particle aerodynamic diameter is less than 2.5 μm) and

PM_{10} (particle aerodynamic diameter is less than 10 μm) are considered as the main pollutants of air pollution and play an important role in regional and urban pollution space [19]. The increase of $PM_{2.5}$ and PM_{10} in mass concentration can increase the extinction coefficient of the atmosphere and reduce the visibility through the atmosphere, leading to the occurrence of smog events, and harm the environment and human health, thus more and more attention has been paid to the study of particulate matters on hazy days [20–24].

The observation study of aerosols is a prerequisite for haze pollution management and prevention. In China, the rapid development of the economy and urbanization construction has led to a large number of anthropogenic pollutant emissions and several haze pollution episodes in recent decades. Scientists have conducted a large number of experimental studies on haze and have achieved many pioneering research results. $PM_{2.5}$ concentrations during smog in Wuhan are 9.9 times higher than those during non-smog periods (333 versus 34 $\mu g \cdot m^{-3}$), which showed that the degree of haze pollution was very serious [25]. Li et al. studied the temporal and spatial distribution of $PM_{2.5}$ and PM_{10} in Shen-yang, Northeast China. The relationship between PM and meteorological factors is discussed [26]. Li et al. used trajectory clustering potential source contribution function (PSCF) and concentration-weighted trajectories (CWT) methods to study transmission paths and potential sources of $PM_{2.5}$ and PM_{10} in each season in Beijing [27]. Tao et al. found that increasing relative humidity can increase $PM_{2.5}$ particle size, increase its extinction characteristics, and reduce visibility. At the same time, increased relative humidity also contributes to $PM_{2.5}$ production [28]. At present, the haze in China is mainly distributed in the Beijing-Tianjin-Hebei region [29,30], the Yangtze River Delta region [31], and the Pearl River Delta region [28,32]; where the economy is developed and the level of anthropogenic pollutants emission is high, haze is responsible for a long-lasting wide range of highly concentrated aerosols.

In recent years, the Central Plains region of China has also experienced rapid economic development and urbanization, and air pollution events have been occurring. Located in Central China, Nanyang is a more developed city in southwestern Henan province and a strategic water source for the Chinese South-North Water Transfer Project. The city, located in the Nanyang Basin, has seen rapid economic development and frequent air pollution incidents in recent years. However, relatively few studies have been conducted on atmospheric particulate matter in Nanyang. Therefore, this study selects Nanyang as the experimental area and focuses on the concentration characteristics of $PM_{2.5}$, PM_{10}, and TSP, and the causes of and the relationship between particulate matter and meteorological factors during winter from 19 November 2021 to 19 March 2022.

2. Materials and Methods

The air quality monitoring station is located in Nanyang, a city with an area of approximately 26,000 km^2 and with a population of approximately 9,713,100 [33] in the southwest of Henan Province. It is at the intersection of the three provinces of Hubei, Henan, and Shanxi as well as the core of the geographic region formed by the three provincial capitals, i.e., Wuhan, Zhengzhou, and Xi'an. The climate is generally moderate and is a four-season humid subtropical climate, with strong monsoon influences: winters are cool but dry, and summers are hot and humid. Spring and autumn provide transitions of reasonable length.

The Nanyang Normal University Station (NYNU) was selected as the experimental site, which is located in the southwest suburb of Nanyang and the left bank area of the Baihe River (Figure 1). The air quality monitoring station comprises a particulate matter monitoring module and a meteorological element monitoring module. The particle monitoring module consists of a 2.5 μm sampling head and a 10 μm sampling head, which can continuously provide real-time measurements of TSP, $PM_{2.5}$, and PM_{10} concentrations using the light scattering method, and data transmission to the background computer for storage. The measuring range of the data is 0–1000 $\mu g/m^3$, and the minimum monitoring limit is ≤ 1 $\mu g/m^3$. The meteorological element module includes five sensors that can provide real-time measurements of temperature, relative humidity, wind direction, wind speed, and air pressure. The measuring accuracy and range are given in Table 1.

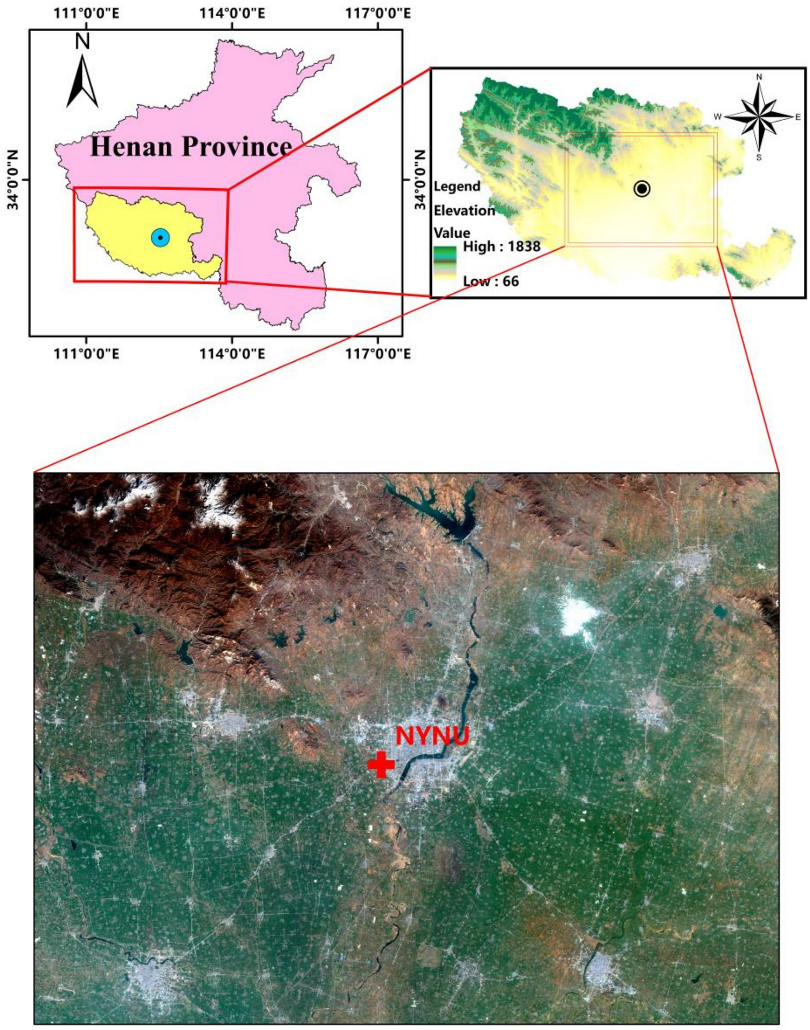

Figure 1. Location of the air quality monitoring station (Latitude: 32°17′ N–33°48′ N; Longitude: 110°58′ E–113°49′ E).

Table 1. The measuring accuracy and range of parameters in the NYNU site.

Parameters	Unit	Accuracy	Range
$PM_{2.5}$	($\mu g/m^3$)	≤ 1	0~1000
PM_{10}	($\mu g/m^3$)	≤ 1	0~1000
TSP	($\mu g/m^3$)	≤ 1	0~1000
WS	($m \cdot s^{-1}$)	± 0.3	0~30
T	(°C)	± 0.3	−30–70
RH	(%)	± 5	0~100

The experimental period is from 19 November 2021 to 19 March 2022, which coincides with the high incidence of haze during winter in Nanyang and is conducive to the in-depth exploration of haze characteristics. In the study, we first used statistical methods to analyze the overall characteristics of PM2.5, PM10, TSP, and the meteorological factors (wind speed, wind direction, temperature, and relative humidity) in winter in Nanyang. Then, the characteristics of the day-to-day variation of these variables are studied, and the relationship between PM2.5, PM10, TSP, and the meteorological factors is discussed.

3. Results and Discussion

3.1. Temporal Behavior of Particulate Matters and Meteorological Factors

The temporal behaviors of $PM_{2.5}$, PM_{10}, TSP, temperature, relative humidity, and wind speed are shown in Figure 2, and the statistical information of the corresponding parameters is given in Table 2. In general, all six physical variables had certain daily cycle features; the features of $PM_{2.5}$, PM_{10}, and TSP were the same, and the mean concentrations of $PM_{2.5}$, PM_{10}, and TSP were 106 $\mu g/m^3$, 137 $\mu g/m^3$, and 283 $\mu g/m^3$, respectively, indicating that concentrations of particulate matter were higher than the Chinese ambient air quality secondary standard (100 $\mu g/m^3$ annual mean for PM_{10}, 35 $\mu g/m^3$ annual mean for $PM_{2.5}$). The standard deviations of $PM_{2.5}$, PM_{10}, and TSP were 57 $\mu g/m^3$, 74 $\mu g/m^3$, and 131 $\mu g/m^3$, respectively, indicating that concentrations of particulate matter had more dramatic changes during the observation period. In January 2018, the mean $PM_{2.5}$ mass concentration in Wuhan was 170 $\mu g/m^3$ during polluted weather, which was higher than the four-month mean $PM_{2.5}$ mass concentration observed in this study [34]. At the NYNU site, a heavy pollution event occurred from 16 to 20 January 2022, and the maximum concentrations of $PM_{2.5}$, PM_{10}, and TSP were 309 $\mu g/m^3$, 399 $\mu g/m^3$, and 747 $\mu g/m^3$, respectively, which were 2.9, 2.9, and 2.6 times, respectively, that of the average concentrations throughout the winter season. This indicates that the mean particulate matter concentrations in the Nanyang area during the severe winter haze were very high. This severe haze event was similar to what was experienced in Wuhan in June 2012, when the $PM_{2.5}$ concentrations reached 333 $\mu g/m^3$, which was 9.9 times higher than the $PM_{2.5}$ mass concentration during normal days [25].

Table 2. Statistics of each variable of particulate matter and meteorology parameters during the experimental period.

Parameters	Unit	Mean	SD	Number	Skewness	Percentiles				
						10%	25%	50%	75%	90%
$PM_{2.5}$	($\mu g/m^3$)	106.47	57.35	2888	1.10	39.60	69.14	96.85	101.90	131.77
PM_{10}	($\mu g/m^3$)	137.32	74.20	2888	1.09	50.76	89.06	125.27	170.23	236.35
TSP	($\mu g/m^3$)	283.40	131.28	2888	1.09	130.27	198.04	262.10	341.61	458.63
WS	($m \cdot s^{-1}$)	0.61	0.53	2888	2.34	0.18	0.26	0.44	0.75	1.30
T	(°C)	5.59	5.04	2888	0.98	0.38	2.21	4.18	8.30	13.98
RH	(%)	73.31	16.54	2888	−0.32	51.62	61.96	73.41	86.56	93.97

Nanyang is located on the dividing line of the zero degrees isotherm in January in China, with an average temperature of 6 °C and average relative humidity of 73% in winter. This indicates that the winter temperature in Nanyang is relatively low and the relative humidity is relatively high. The lower temperature is not conducive to atmospheric convection, resulting in a lower atmospheric boundary layer height and an increase in particulate matter concentration [35]. The higher relative humidity is conducive to the hygroscopic growth of aerosols, which increases concentration. The higher relative humidity is also conducive to the occurrence of optical secondary reactions of polluting gases and the formation of new aerosol particles, which also increases the particulate matter mass concentration and aggravates the air pollution level. At the same time, the average wind speed (WS) was lower (1 m/s), and the main prevailing wind direction was southeast (26% relative frequency) and east (22.5% relative frequency) (Figure 3). This could be related to the topography of Nanyang as it belongs to the basin terrain, surrounded by mountains on three sides (Qinling mountain range in the northwest, Fuyu mountain range in the north, and fewer mountains in the southwest). Low wind speed is not conducive to the transport and dispersion of pollutants, which might contribute to haze pollution events. Therefore, the meteorological and topographical factors of Nanyang could be one of the triggers for the local haze pollution events.

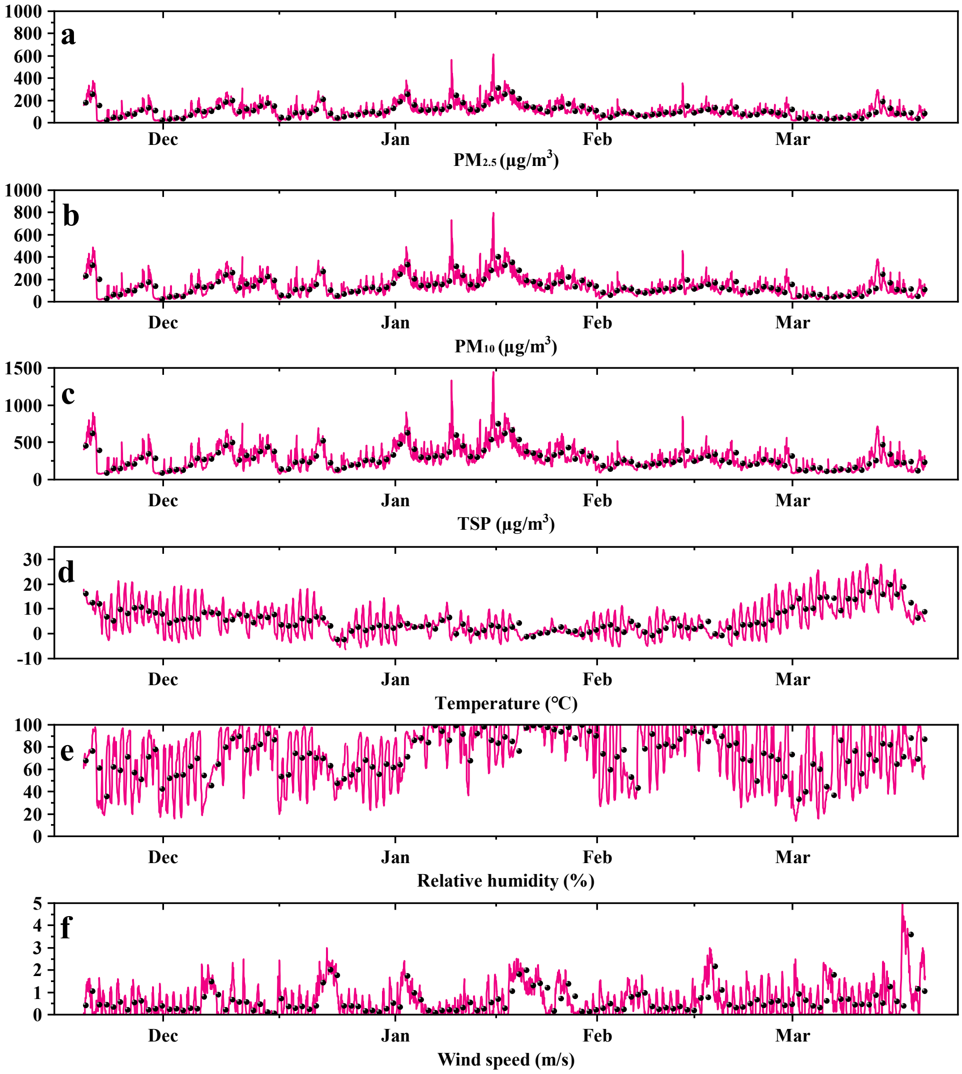

Figure 2. Time series of each variable over the whole experimental period (red line), black dots indicate the daily average of the parameters: (**a**) $PM_{2.5}$ (μg/m^3); (**b**) PM_{10} (μg/m^3); (**c**) TSP (μg/m^3); (**d**) Temperature (°C); (**e**) Humidity (%); (**f**) Windspeed (m/s).

Figure 4 shows the relative frequency and cumulative frequency distribution of each variable of particulate matter and meteorology during the experimental period. Skewness is a measure of the direction and degree of skewness of the data distribution, indicating the degree of asymmetry of the density curve of the probability distribution relative to the mean, which intuitively appears to be the relative length of the tail of the density function curve. The normal distribution has a skewness of zero; there is a positive skewness if the data distribution is skewed to the left, and a negative skewness if the data distribution is skewed to the right. As given in Table 2, skewness values of $PM_{2.5}$, PM_{10}, TSP, WS, T, and RH were 1.10, 1.09, 1.09, 2.34, 0.98, −0.32, respectively, indicating that distributions of all variables are skewed to the left, except for the relative humidity, which is skewed to the right. As shown in Figure 5, concentrations of $PM_{2.5}$ were mainly concentrated in the range of 25~150 μg/m^3, with a relative frequency of 75%; concentrations of PM_{10} were mainly concentrated in the range of 25~200 μg/m^3, with a relative frequency of 79%; concentrations of TSP were mainly concentrated in the range of 100~375 μg/m^3, with a relative frequency of 79%. The distribution of T (°C) was mainly concentrated between −2.5~10 °C, with a relative frequency of 86%; RH (%) is mainly concentrated between 80%~100%, with a relative frequency of 54%, indicating that the relative humidity is high during winter.

WS (m/s) is mainly concentrated between 0~0.5 m/s, with a relative frequency of 56%, indicating a low wind speed value during winter.

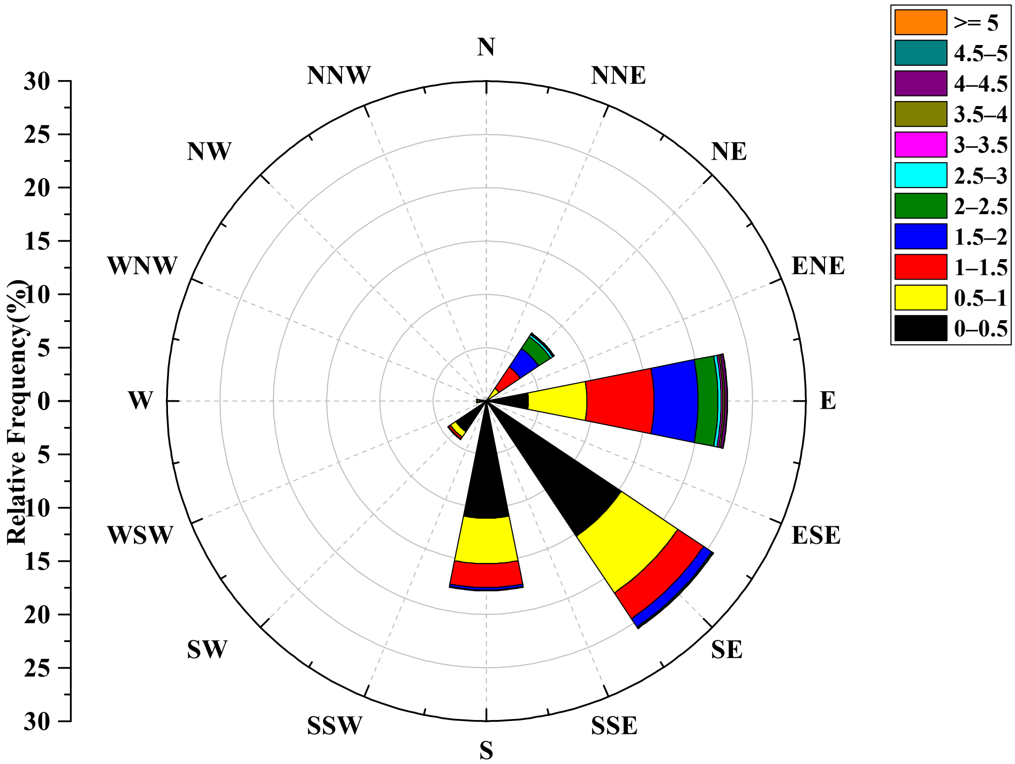

Figure 3. Wind speed and direction rises at the NYNU site in Nanyang from 19 November 2021 to 19 March 2022.

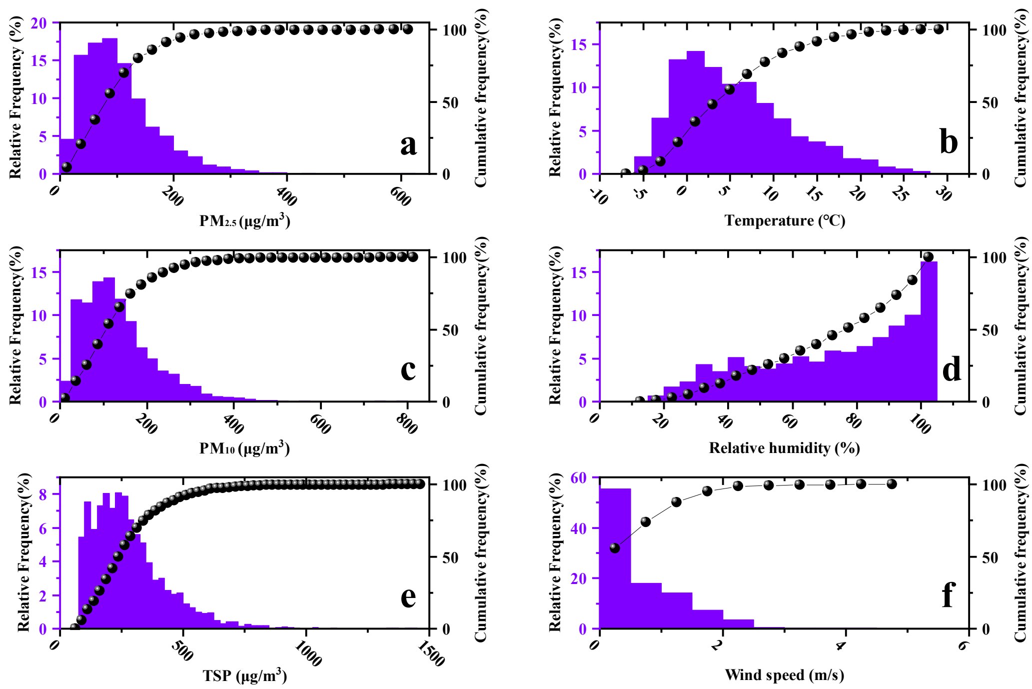

Figure 4. Relative and cumulative frequency distributions of the variables over the entire experimental period: (**a**) $PM_{2.5}$; (**b**) Temperature; (**c**) PM_{10}; (**d**) Relative Humidity; (**e**) TSP; (**f**) Wind speed.

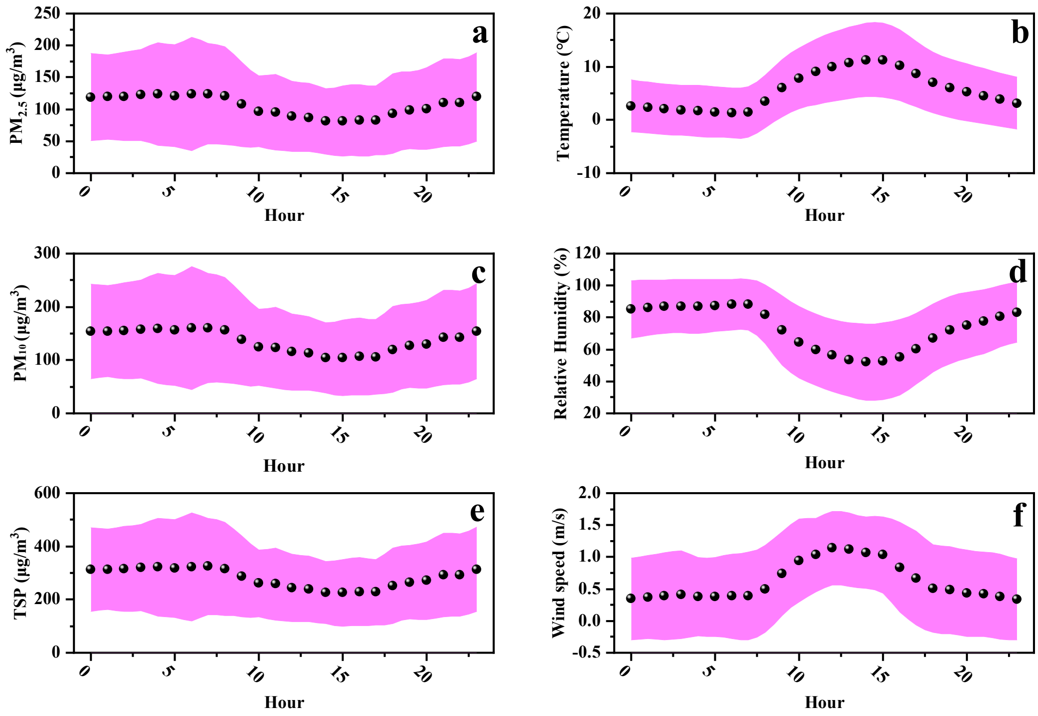

Figure 5. Daily trends of each variable at the NYNU station during the experimental cycle. Black dots represent the mean and red areas represent the standard deviation of (**a**) $PM_{2.5}$ (μg/m^3); (**b**) Temperature (°C); (**c**) PM_{10} (μg/m^3); (**d**) Humidity (%); (**e**) Total suspended particulate matter TSP (μg/m^3); (**f**) Windspeed (m/s).

Table 3 presents $PM_{2.5}$ and PM_{10} concentrations observed at several stations in China, including urban and rural stations. The mean and standard deviation of $PM_{2.5}$ and PM_{10} in winter at the NYNU site were 106 ± 57μg/m^3 and 137 ± 74 μg/m^3, respectively. As mentioned, $PM_{2.5}$ and PM_{10} concentrations exceeded the Chinese national secondary standard, which was nearly equivalent to the concentrations in Beijing (108 μg/m^3 for $PM_{2.5}$, 172 μg/m^3 for PM_{10}) [32], but was lower than other major cities during periods of haze pollution, such as Wuhan (170 μg/m^3 for $PM_{2.5}$) [34] and Nanjing (222 μg/m^3 for $PM_{2.5}$, 316 μg/m^3 for PM_{10}) [36]. This suggests that the air pollution level in Nanyang city was comparably moderate. The mean $PM_{2.5}/PM_{10}$ ratio of 0.77 indicates the presence of mainly $PM_{2.5}$ compared to PM_{10}, and this result is consistent with the findings of Zhang et al. [33]. The mean value of $PM_{2.5}/PM_{10}$ in mainland Chinese cities was 0.67, which is also similar to our result [37].

Table 3. Comparison of particulate matter mass concentration between NYNU station and other regional stations.

SITE	TYPE	PERIOD	SEASON	$PM_{2.5}$ (μg/m^3)	PM_{10} (μg/m^3)	Reference
NYNU (China)	urban	November 2021–March 2022	Winter	106 ± 57	137 ± 74	This work
Taocha (China)	rural	October 2018–September 2019	Annual	51 ± 22	57 ± 25	[33]
Wuhan (China)	urban	18–21 January 2018	Winter	170	——	[34]
Shenyang (China)	urban	2014–2015	Annual	72	118	[26]
Nanjing (China)	urban	2001	Annual	222	316	[36]
Chengdu (China)	urban	2009–2011	Annual	60	71	[38]
Hongkong (China)	urban	January 2000–December 2001	Winter	50.2	78.9	[39]
Shanghai (China)	urban	January 2004–December 2005	Winter	68	118	[40]
Beijing (China)	urban	September 2017–August 2019	Annual	108	172	[32]
Guangzhou (China)	urban	March 2013–February 2014	Annual	52	73	[32]

3.2. Diurnal Variation of Particle Concentrations and Meteorological Factors

Figure 5 shows the daily variability of each variable at the NYNU monitoring station during the experimental period. From Figure 5a,c,e, it can be seen that the concentrations of $PM_{2.5}$, PM_{10}, and TSP peaked from 7:00 a.m. to 8:00 a.m. with 124 μg/m^3, 160 μg/m^3, and 324 μg/m^3, respectively. The NYNU monitoring station was located near the commercial area of Wolong Road, and staff would come to work on campus from 7:00 a.m. to 8:00 a.m. The morning rush hour and enhanced commercial activities led to the discharge of pollutants in the morning [41]. In addition, relative humidity also reaches the maximum value (88%) during the morning (7:00 a.m. to 8:00 a.m.). The increase in relative humidity might be responsible for photochemical reactions and the generation of secondary aerosol particulate matter, which could also increase aerosol concentrations. At the same time, the low wind speed (~0.5 m/s) in the morning causes a continuous accumulation of particulate matter. $PM_{2.5}$, PM_{10}, and TSP begin to decrease after the morning peak and reach the lowest value level of 81 μg/m^3, 105 μg/m^3, and 226 μg/m^3, respectively, at 14:00–18:00 local time. The reason could mainly be that the temperature rises from 14:00–18:00 and the wind speed accelerates, which leads to the atmospheric boundary layer being lifted, diluting the concentration of particulate matter [27]; similarly, particulate matter was also blown away by the increased wind speed. The relative humidity also reached the minimum of the day (52%) from 14:00 to 18:00, the secondary aerosol production efficiency decreased, and the mass concentration of particulate matter decreased. At 18:00–24:00, the concentration of particulate matter gradually increased, and was maintained at a very high level from 0:00 to 8:00 a.m., which was mainly due to the lower temperature and lower altitude of the atmospheric boundary layer at night, leading aerosols to gather in the lower space. At the same time, during the night time, the wind speed also gradually weakened, which was not conducive to the dispersion of particulate matter, increasing particulate matter concentrations.

3.3. Relationship between Particulate Matter Concentrations and Meteorological Parameters

The relationships between mass concentrations of $PM_{2.5}$, PM_{10}, TSP, and temperature, relative humidity, and wind speed are shown in Figure 6. By studying the relationship between the concentration of particulate matter and meteorological factors, we can identify the main influencing factors that affect the mass concentration of particulate matter in the atmosphere. As shown in Figure 6, each small red dot on the graph represents the daily average value of each variable. In Figure 6, the correlation coefficients (R) of temperature, humidity, and wind speed with $PM_{2.5}$, PM_{10}, and TSP are −0.17, −0.17, −0.17, 0.53, 0.53, 0.53, and 0.10, 0.10, 0.10, respectively, indicating that the values of $PM_{2.5}$, PM_{10}, and TSP show a weak negative correlation with temperature, a relatively strong positive correlation with humidity, and a weak positive correlation with wind speed. Therefore, relative humidity is the most important influencing factor on the mass concentration of particulate matter during winter for the NYNU site. The increase in relative humidity could induce photochemical reactions and produce secondary aerosol particulate matter in the atmosphere. In winter, the temperature and wind speed at NYNU were always low, so the temperature and wind speed have little influence on PM mass concentrations. In the study of Bai et al., when RH reached 90–100% high values, the aerosol scattering coefficient, absorption coefficient, extinction coefficient, and SSA are also at high values, indicating that high relative humidity can promote the formation of PM [34]. Similarly, in the study of Zhang et al., a high correlation was found between relative humidity and PM mass concentration at the TC suburban site, which is mainly due to the high relative humidity that accelerated the photochemical reaction in the atmosphere, generating secondary aerosols in winter [33]. Similar results were also found in other cities, such as Beijing [27,42], Shanghai [40,43], and Guangzhou [28,44].

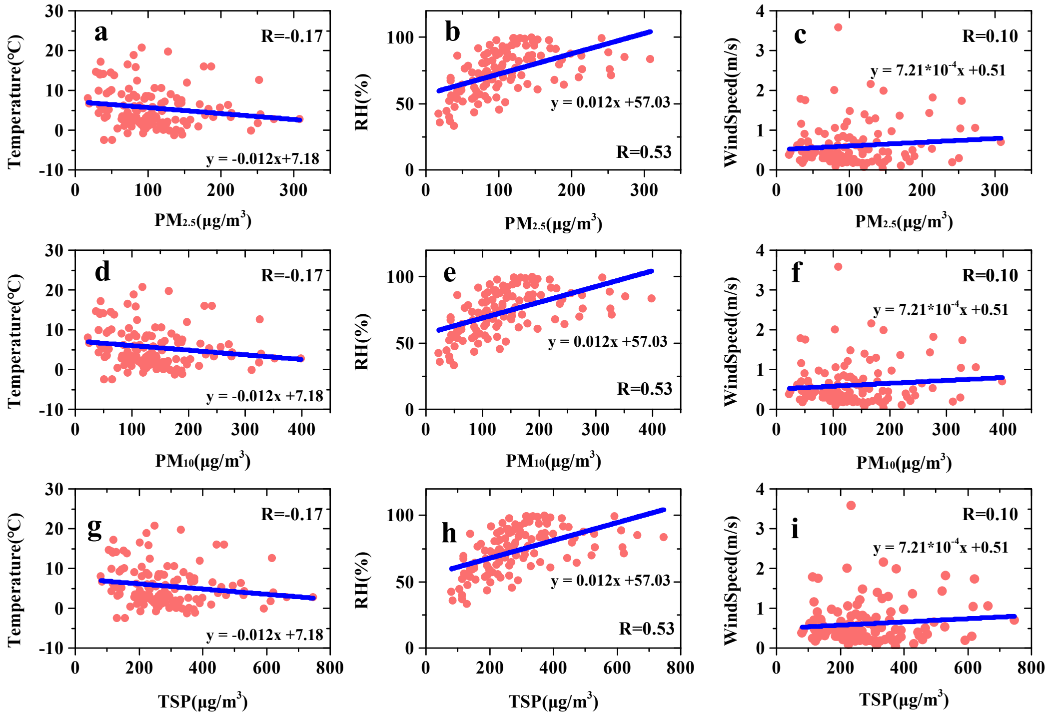

Figure 6. Correlation analysis of $PM_{2.5}$, PM_{10}, TSP, and meteorological elements during the experimental cycle: (**a**) $PM_{2.5}$ and temperature; (**b**) $PM_{2.5}$ and humidity; (**c**) $PM_{2.5}$ and wind speed; (**d**) PM_{10} and temperature; (**e**) PM_{10} and humidity; (**f**) PM_{10} and wind speed; (**g**) TSP and temperature; (**h**) TSP and humidity; (**i**) TSP and wind speed.

4. Conclusions

To investigate the characteristics of winter aerosols in Nanyang (China) and their influencing factors, we conducted a four-month observation experiment at the NYNU station of Nanyang Normal University to deeply investigate the relationship between winter aerosols and meteorological parameters. This study can provide theoretical support and valuable data support for government decision-makers as well as related researchers. The relevant conclusions are as follows:

(1) During the whole experimental cycle, the overall concentrations of $PM_{2.5}$, PM_{10}, and TSP monitored at this site were 106 ($\mu g/m^3$), 137 ($\mu g/m^3$), and 283 ($\mu g/m^3$), respectively, on average. The number of days that meet the national secondary standard 24-h average mass concentration of $PM_{2.5}$ accounts for approximately 30%, PM_{10} accounts for approximately 64%, and TSP accounts for approximately 64%. The sources and distribution of aerosols in Nanyang are mainly determined by anthropogenic emissions, such as dust from industrial and agricultural production, waste gas from fossil fuel combustion, and vehicle exhaust from transportation.

(2) The mass concentrations of $PM_{2.5}$, PM_{10}, and TSP at NYNU station are mainly due to commercial activities and vehicle emissions. At the NYNU station, the type of particulate matter is dominated by fine particulate matter ($PM_{2.5}$). Meanwhile, the mass concentrations of $PM_{2.5}$, PM_{10}, and TSP at NYNU station are mainly concentrated in the morning from 7:00 to 8:00 a.m. LT due to the increase of pollutant emissions in the morning rush hour.

(3) The mass concentrations of $PM_{2.5}$, PM_{10}, and TSP in Nanyang in winter showed significant positive correlations with relative humidity and weak correlations with temperature and wind speed. This suggests that higher relative humidity in Nanyang in winter could increase the formation of particulate matter.

Author Contributions: Conceptualization, M.Z.; methodology, M.Z. and S.C.; software, S.G., F.Z. and Y.W.; validation, J.C., X.Z. and P.Q.; formal analysis, M.Z.; investigation, M.Z. and M.B.; resources, M.Z.; data curation, M.Z.; writing—original draft preparation, M.Z.; writing—review and editing, M.B. and M.C.; visualization, M.Z.; supervision, F.L.; project administration, M.Z.; funding acquisition, M.Z. All authors have read and agreed to the published version of the manuscript.

Funding: This research was funded by the Key Scientific Research Project of Henan institutions of higher learning, grant number 22B170004; the Nanyang Normal University Scientific Research Project, grant number 2020QN033.

Institutional Review Board Statement: Not applicable.

Informed Consent Statement: Not applicable.

Data Availability Statement: Not applicable.

Acknowledgments: We thank the editors for assisting in the linguistic refinement of this manuscript.

Conflicts of Interest: The authors declare no conflict of interest.

References

1. Kaufman, Y.J.; Tanré, D.; Boucher, O. A satellite view of aerosols in the climate system. *Nature* **2002**, *419*, 215–223. [CrossRef]
2. Ramanathan, V.; Crutzen, P.J.; Kiehl, J.T.; Rosenfeld, D. Aerosols, Climate, and the Hydrological Cycle. *Science* **2001**, *294*, 2119–2124. [CrossRef]
3. Jocelyn, K.; Granmar, M. Mounting Evidence Indicts Fine-Particle Pollution. *Science* **2005**, *307*, 1858–1861.
4. Jacobson, M.Z. Strong radiative heating due to the mixing state of black carbon in atmospheric aerosols. *Nature* **2001**, *409*, 695–697. [CrossRef]
5. Edenhofer, O. *Climate Change 2014: Mitigation of Climate Change: Working Group Iii Contribution to the Fifth Assessment Report of the Intergovernmental Panel on Climate Change*; Cambridge University Press: Cambridge, UK, 2014.
6. Cappa, C.D.; Onasch, T.B.; Massoli, P.; Worsnop, D.R.; Bates, T.S.; Cross, E.S.; Davidovits, P.; Hakala, J.; Hayden, K.L.; Jobson, B.T.; et al. Radiative Absorption Enhancements Due to the Mixing State of Atmospheric Black Carbon. *Science* **2012**, *337*, 1078. [CrossRef] [PubMed]
7. Kulmala, M.; Kontkanen, J.; Junninen, H.; Lehtipalo, K.; Manninen, H.E.; Nieminen, T.; Petäjä, T.; Sipilä, M.; Schobesberger, S.; Rantala, P.; et al. Direct Observations of Atmospheric Aerosol Nucleation. *Science* **2013**, *339*, 943–946. [CrossRef]
8. Ackerman, A.S.; Kirkpatrick, M.P.; Stevens, D.E.; Toon, O.B. The impact of humidity above stratiform clouds on indirect aerosol climate forcing. *Nature* **2004**, *432*, 1014–1017. [CrossRef] [PubMed]
9. Albrecht, B.A. Aerosols, Cloud Microphysics, and Fractional Cloudiness. *Science* **1989**, *245*, 1227–1230. [CrossRef]
10. Crutzen, P.J.; Andreae, M.O. Biomass Burning in the Tropics: Impact on Atmospheric Chemistry and Biogeochemical Cycles. *Science* **1990**, *250*, 1669–1678. [CrossRef] [PubMed]
11. Meng, Z.; Dabdub, D.; Seinfeld, J.H. Chemical Coupling Between Atmospheric Ozone and Particulate Matter. *Science* **1997**, *277*, 116–119. [CrossRef]
12. Shi, T.; Han, G.; Ma, X.; Gong, W.; Chen, W.; Liu, J.; Zhang, X.; Pei, Z.; Gou, H.; Bu, L. Quantifying CO_2 Uptakes Over Oceans Using LIDAR: A Tentative Experiment in Bohai Bay. *Geophys. Res. Lett.* **2021**, *48*, e2020GL091160. [CrossRef]
13. Shi, T.; Han, G.; Ma, X.; Zhang, M.; Pei, Z.; Xu, H.; Qiu, R.; Zhang, H.; Gong, W. An inversion method for estimating strong point carbon dioxide emissions using a differential absorption Lidar. *J. Clean. Prod.* **2020**, *271*, 122434. [CrossRef]
14. Pei, Z.; Han, G.; Ma, X.; Shi, T.; Gong, W. A Method for Estimating the Background Column Concentration of CO_2 Using the Lagrangian Approach. *IEEE Trans. Geosci. Remote Sens.* **2022**, *60*, 1–12. [CrossRef]
15. Qiu, R.; Li, X.; Han, G.; Xiao, J.; Ma, X.; Gong, W. Monitoring drought impacts on crop productivity of the U.S. Midwest with solar-induced fluorescence: GOSIF outperforms GOME-2 SIF and MODIS NDVI, EVI, and NIRv. *Agric. For. Meteorol.* **2022**, *323*, 109038. [CrossRef]
16. Kaiser, J. How Dirty Air Hurts the Heart. *Science* **2005**, *307*, 1858–1859. [CrossRef]
17. Huang, R.J.; Zhang, Y.; Bozzetti, C.; Ho, K.F.; Cao, J.J.; Han, Y.; Daellenbach, K.R.; Slowik, J.G.; Platt, S.M.; Canonaco, F.; et al. High secondary aerosol contribution to particulate pollution during haze events in China. *Nature* **2014**, *514*, 218–222. [CrossRef]
18. Zhang, Q.; Jiang, X.; Tong, D.; Davis, S.J.; Zhao, H.; Geng, G.; Feng, T.; Zheng, B.; Lu, Z.; Streets, D.G.; et al. Transboundary health impacts of transported global air pollution and international trade. *Nature* **2017**, *543*, 705–709. [CrossRef]
19. Ambade, B. Characterization of PM_{10} over Urban and Rural Sites of Rajnandgaon, Central India. *Nat. Hazards* **2016**, *80*, 589–604. [CrossRef]
20. Ding, A.; Huang, X.; Nie, W.; Chi, X.; Xu, Z.; Zheng, L.; Xu, Z.; Xie, Y.; Qi, X.; Shen, Y.; et al. Significant Reduction of $PM_{2.5}$ in Eastern China Due to Regional-Scale Emission Control: Evidences from the Sorpes Station, 2011–2018. *Atmos. Chem. Phys.* **2019**, *19*, 11791–11801. [CrossRef]
21. Cao, J.; Xu, H.; Xu, Q.; Chen, B.; Kan, H. Fine Particulate Matter Constituents and Cardiopulmonary Mortality in a Heavily Polluted Chinese City. *Environ. Health Perspect.* **2012**, *120*, 373–378. [CrossRef]

22. Ding, A.; Nie, W.; Huang, X.; Chi, X.; Sun, J.; Kerminen, V.-M.; Xu, Z.; Guo, W.; Petäjä, T.; Yang, X.; et al. Long-term observation of air pollution-weather/climate interactions at the SORPES station: A review and outlook. *Front. Environ. Sci. Eng.* **2016**, *10*, 15. [CrossRef]
23. Wang, R.K.; Pathak, W.S.; Wu, T. Summertime $PM_{2.5}$ Ionic Species in Four Major Cities of China: Nitrate Formation in an Ammonia-Deficient Atmosphere. *Atmos. Chem. Phys.* **2009**, *9*, 1711–1722.
24. Basant, S.; Balram, A. Review on Composition, Emission Sources of Rspm, Tspm, Heavy Metals and Ions with Effect on Environment and Health. *Res. J. Chem. Environ.* **2016**, *20*, 31–43.
25. Zhang, M.; Ma, Y.; Gong, W.; Zhu, Z. Aerosol Optical Properties of a Haze Episode in Wuhan Based on Ground-Based and Satellite Observations. *Atmosphere* **2014**, *5*, 699–719. [CrossRef]
26. Li, X.; Ma, Y.; Wang, Y.; Liu, N.; Hong, Y. Temporal and spatial analyses of particulate matter (PM_{10} and $PM_{2.5}$) and its relationship with meteorological parameters over an urban city in northeast China. *Atmos. Res.* **2017**, *198*, 185–193. [CrossRef]
27. Li, D.; Cheng, Y.; Liu, J.; Zhang, J.; Gui, H.; Du, P.; Yu, T.; Wang, J.; Lu, Y.; Liu, W. Identification of Long-Range Transport Pathways and Potential Sources of $PM_{2.5}$ and PM_{10} in Beijing from 2014 to 2015. *J. Environ. Sci.* **2017**, *56*, 214–229. [CrossRef]
28. Tao, J.; Zhang, L.; Zhang, Z.; Huang, R.; Wu, Y.; Zhang, R.; Cao, J.; Zhang, Y. Control of $PM_{2.5}$ in Guangzhou during the 16th Asian Games period: Implication for hazy weather prevention. *Sci. Total. Environ.* **2015**, *508*, 57–66. [CrossRef]
29. He, K.; Yang, F.; Ma, Y.; Zhang, Q.; Yao, X.; Chan, C.K.; Cadle, S.; Chan, T.; Mulawa, P. The Characteristics of $PM_{2.5}$ in Beijing, China. *Atmos. Environ.* **2001**, *35*, 4959–4970. [CrossRef]
30. Lang, J.; Zhang, Y.; Zhou, Y.; Cheng, S.; Chen, D.; Guo, X.; Chen, S.; Li, X.; Xing, X.; Wang, H. Trends of $PM_{2.5}$ and Chemical Composition in Beijing, 2000–2015. *Aerosol Air Qual. Res.* **2017**, *17*, 412–425. [CrossRef]
31. Ding, A.J.; Fu, C.B.; Yang, X.Q.; Sun, J.N.; Zheng, L.F.; Xie, Y.N.; Herrmann, E.; Nie, W.; Petäjä, T.; Kerminen, V.-M.; et al. Ozone and fine particle in the western Yangtze River Delta: An overview of 1 yr data at the SORPES station. *Atmospheric Meas. Tech.* **2013**, *13*, 5813–5830. [CrossRef]
32. Zhang, H.; Wang, Y.; Hu, J.; Ying, Q.; Hu, X.-M. Relationships between meteorological parameters and criteria air pollutants in three megacities in China. *Environ. Res.* **2015**, *140*, 242–254. [CrossRef] [PubMed]
33. Zhang, M.; Wu, D.; Su, B.; Bilal, M.; Li, Y.; Li, B.L. Spatio-Temporal Characteristics of $PM_{2.5}$, PM_{10}, and Aod over Canal Head Taocha Station, Henan Province. *Remote Sens.* **2020**, *12*, 3432. [CrossRef]
34. Bai, D.; Wang, H.; Tan, Y.; Yin, Y.; Wu, Z.; Guo, S.; Shen, L.; Zhu, B.; Wang, J.; Kong, X. Optical Properties of Aerosols and Chemical Composition Apportionment under Different Pollution Levels in Wuhan during January 2018. *Atmosphere* **2019**, *11*, 17. [CrossRef]
35. Bilal, M.; Mhawish, A.; Nichol, J.E.; Qiu, Z.; Nazeer, M.; Ali, M.A.; de Leeuw, G.; Levy, R.C.; Wang, Y.; Chen, Y.; et al. Air Pollution Scenario over Pakistan: Characterization and Ranking of Extremely Polluted Cities Using Long-Term Concentrations of Aerosols and Trace Gases. *Remote Sens. Environ.* **2021**, *264*, 112617. [CrossRef]
36. Wang, G.; Wang, H.; Yu, Y.; Gao, S.; Feng, J.; Gao, S.; Wang, L. Chemical Characterization of Water-Soluble Components of PM_{10} and $PM_{2.5}$ Atmospheric Aerosols in Five Locations of Nanjing, China. *Atmos. Environ.* **2003**, *37*, 2893–2902. [CrossRef]
37. Ma, Y.; Wang, Z.; Tan, Y.; Xu, S.; Kong, S.; Wu, G.; Wu, X.; Li, H. Comparison of Inorganic Chemical Compositions of Atmospheric Tsp, PM_{10} and $PM_{2.5}$ in Northern and Southern Chinese Coastal Cities. *J. Environ. Sci.* **2017**, *55*, 339–353. [CrossRef] [PubMed]
38. Li, Y.; Chen, Q.; Zhao, H.; Wang, L.; Tao, R. Variations in PM_{10}, $PM_{2.5}$ and $PM_{1.0}$ in an Urban Area of the Sichuan Basin and Their Relation to Meteorological Factors. *Atmosphere* **2015**, *6*, 150–163. [CrossRef]
39. Ho, K.F.; Lee, S.C.; Chan, C.K.; Jimmy, C.Y.; Chow, J.C.; Yao, X.H. Characterization of Chemical Species in $PM_{2.5}$ and PM_{10} Aerosols in Hong Kong. *Atmos. Environ.* **2003**, *37*, 31–39. [CrossRef]
40. Chen, J.; Tan, M.; Li, Y.; Zheng, J.; Zhang, Y.; Shan, Z.; Zhang, G.; Li, Y. Characteristics of Trace Elements and Lead Isotope Ratios in $PM_{2.5}$ from Four Sites in Shanghai. *J. Hazard. Mater.* **2008**, *156*, 36–43. [CrossRef]
41. Gong, W.; Zhang, M.; Han, G.; Ma, X.; Zhu, Z. An Investigation of Aerosol Scattering and Absorption Properties in Wuhan, Central China. *Atmosphere* **2015**, *6*, 503–520. [CrossRef]
42. Wang, Y.; Yu, M.; Wang, Y.; Tang, G.; Song, T.; Zhou, P.; Liu, Z.; Hu, B.; Ji, D.; Wang, L.; et al. Rapid formation of intense haze episodes via aerosol–boundary layer feedback in Beijing. *Atmospheric Meas. Tech.* **2020**, *20*, 45–53. [CrossRef]
43. Xu, J.; Tao, J.; Zhang, R.; Cheng, T.; Leng, C.; Chen, J.; Huang, G.; Li, X.; Zhu, Z. Measurements of surface aerosol optical properties in winter of Shanghai. *Atmospheric Res.* **2012**, *109–110*, 25–35. [CrossRef]
44. Andreae, M.O.; Schmid, O.; Yang, H.; Chand, D.; Yu, J.Z.; Zeng, L.-M.; Zhang, Y.-H. Optical properties and chemical composition of the atmospheric aerosol in urban Guangzhou, China. *Atmospheric Environ.* **2008**, *42*, 6335–6350. [CrossRef]